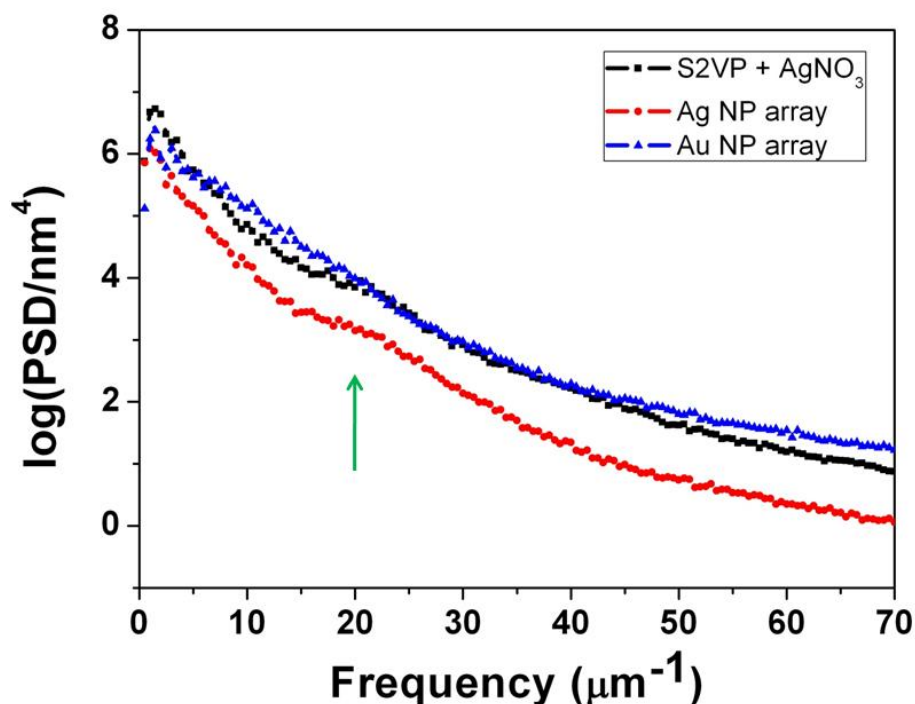## Supporting Information

Controlling the Composition of Plasmonic Nanoparticle Arrays via Galvanic Displacement Reactions on Block Copolymer Nanotemplates

Ji Yong Lee,[a] Jieun Lee,[a] Yu Jin Jang,[a] Juyon Lee,[a] Yoon Hee Jang,[a] Saji Thomas Kochuveedu,[a] Cheolmin Park[b] and Dong Ha Kim[a*]

[a] *Department of Chemistry and Nano Science, Division of Molecular and Life Sciences, College of Natural Sciences, Ewha Womans University, 11-1 Daehyun-dong, Seodaemun-gu, Seoul 120-750, Korea*
[b] *Department of Materials Science and Engineering, Yonsei University, Seoul 120-749, Korea*
E-mail: dhkim@ewha.ac.kr   Fax: +82-2-3277-3419; Tel: +82-2-3277-4517

	S2VP + AgNO₃	Ag NP array	Au NP array
Period	47.5 nm	50 nm	53 nm

Figure S1. Power spectral density profiles calculated from the AFM images ($2 \times 2 \ \mu m^2$) in Figure 1.
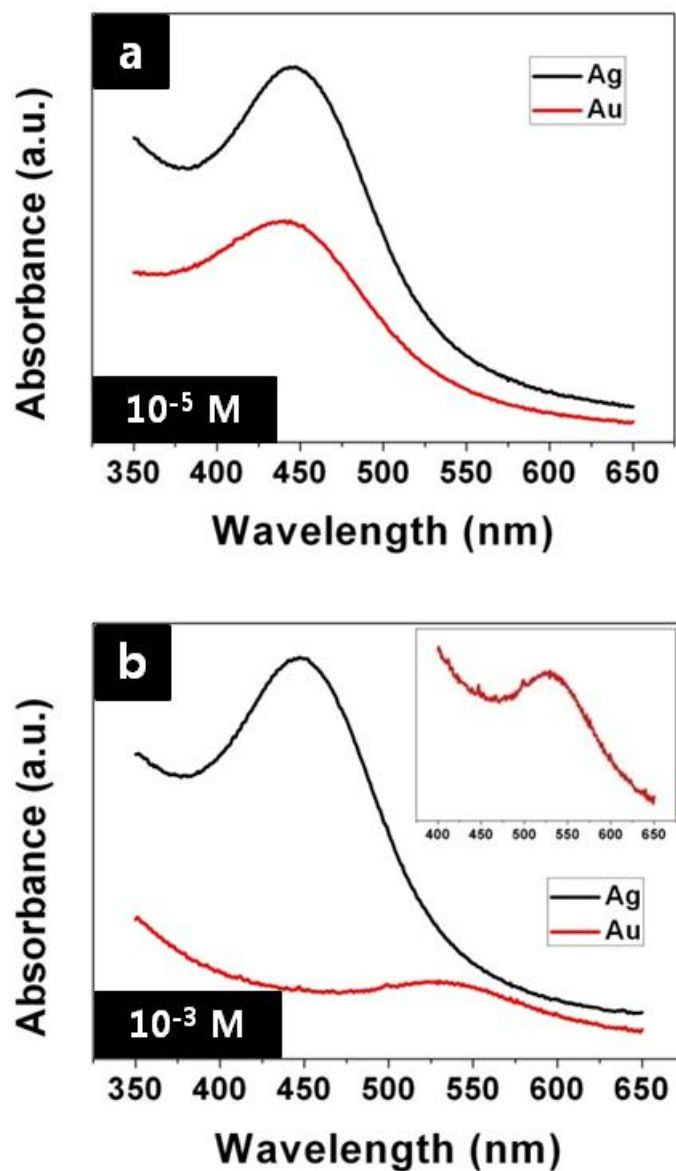
Figure S2. UV-visible absorption spectra obtained from the samples in Figure 1 before (black curves) and after (red ones) applying GDR at a solution concentration of (a) 10^{-5} *M* and (b) 10^{-3} *M*, respectively, at a fixed immersion time of 30 min. Inset in Fig. S2(b) is the magnified view around the characteristic Au peak. Note that the GDR effectively takes place at a solution concentration higher than 10^{-4} *M*.
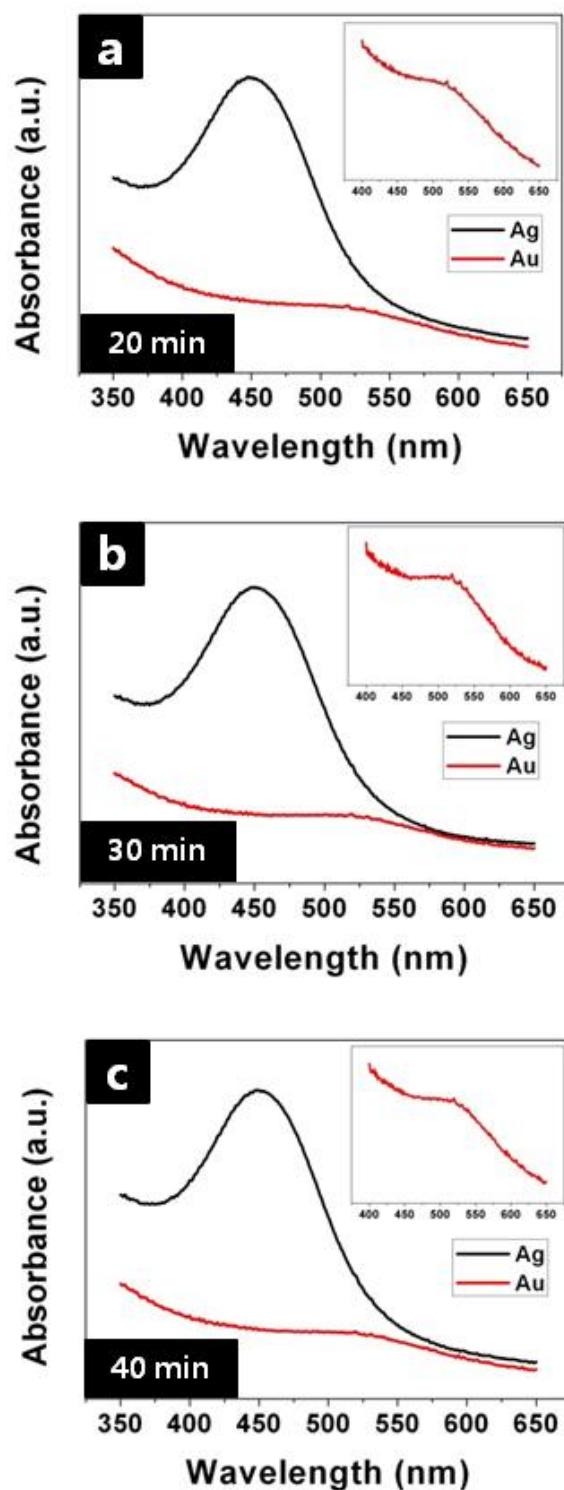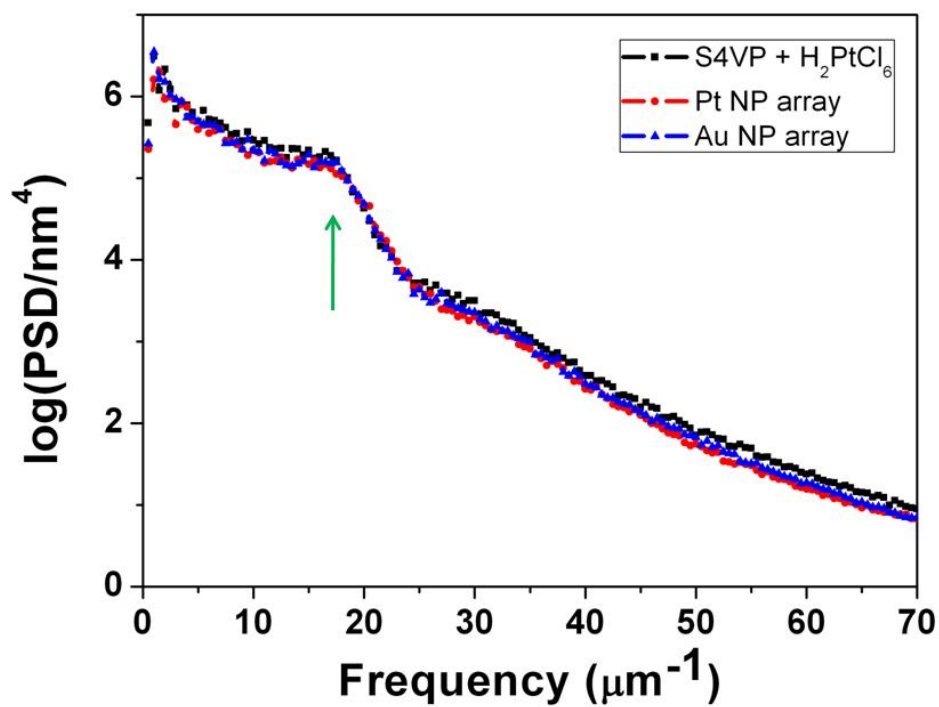
Figure S3. UV-visible absorption spectra obtained from the samples in Figure 1 after applying GDRs in a HAuCl$_4$ solution of 10^{-4} *M* concentration at an immersion time of (a) 20 min, (b) 30 min, and (c) 40 min, respectively. Insets are the magnified view around the characteristic Au peak.

	S4VP + H₂PtCl₆	Pt NP array	Au NP array
Period	59 nm	57 nm	59 nm

Figure S4. Power spectral density profiles calculated from the AFM images (2×2 μm^2) in Figure 5.
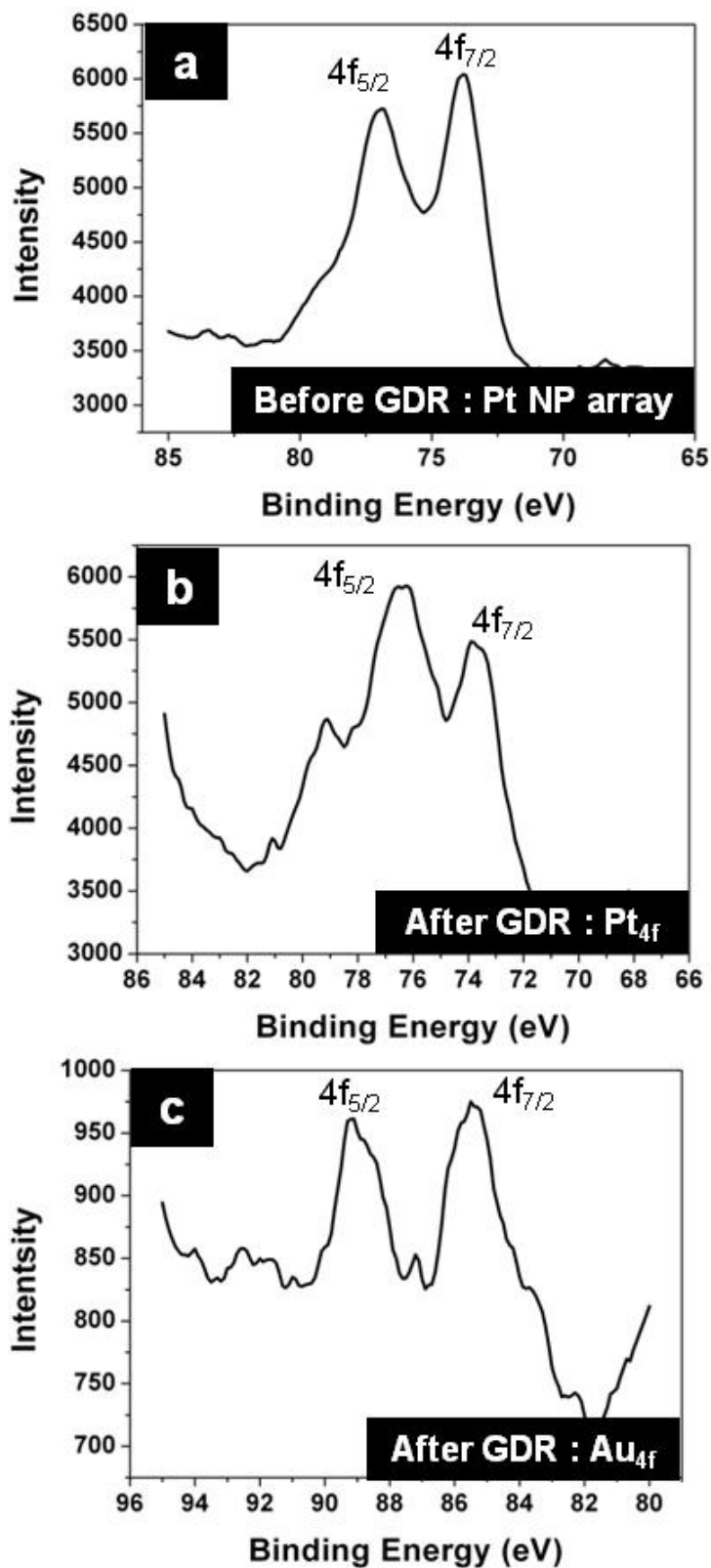
Figure S5. High resolution XPS spectra of (a) Pt_{4f} obtained from the film embedded with Pt NPs in Figure 5(b), (b) Pt_{4f} obtained from the resultant film after GDRs in Figure 5(c), and (c) Au_{4f} obtained from the resultant film after GDRs in Figure 5(c).
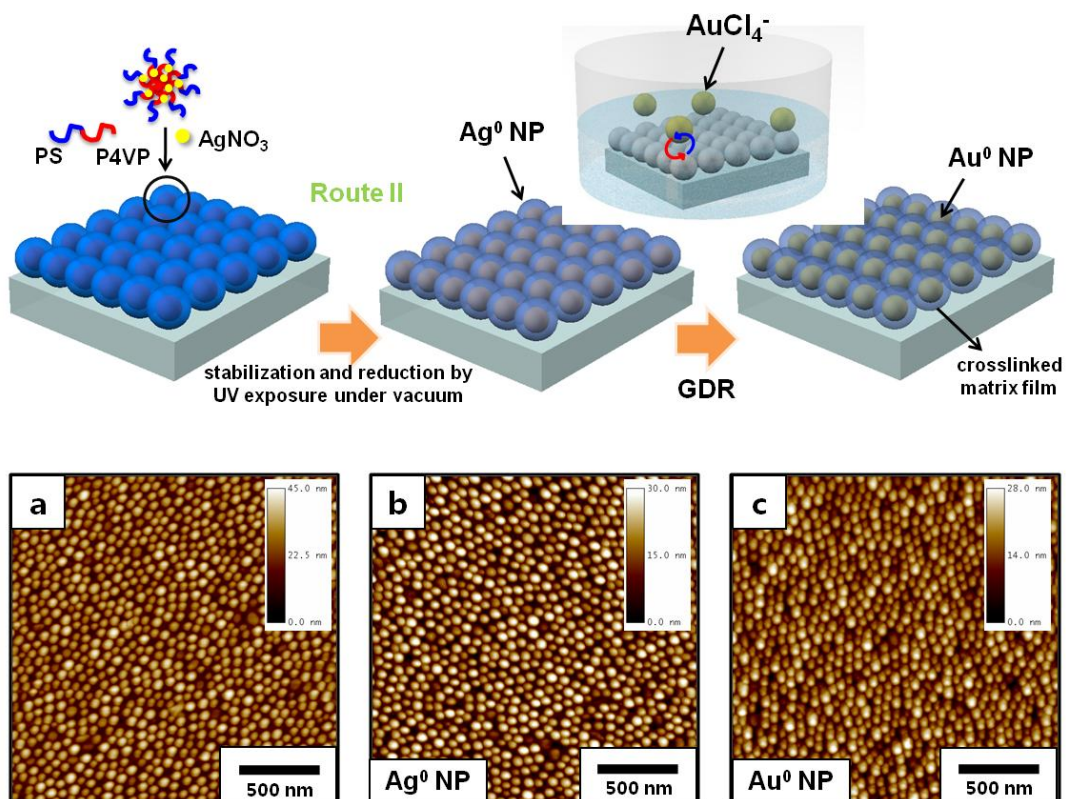
Figure S6. (upper panel) Schematic representation of the process to generate Au NP arrays by converting Ag NPs to Au NPs by applying GDRs in the presence of the polymer shell. (bottom panel) (a) Height contrast AFM images of a PS-*b*-P4VP inverse micelle monolayer containing $AgNO_3$ in the P4VP core; (b) Ag NP arrays embedded in the polymer matrix film obtained by exposing the identical film in Fig. S6(a) to UV light under vacuum environment; (c) Au NP arrays obtained by applying a GDR on the Ag NP arrays in Fig. S6(b).
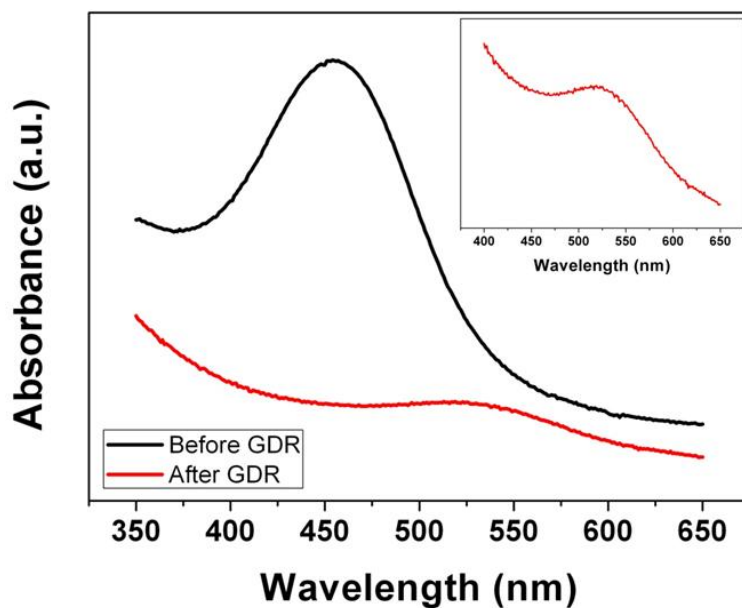
Figure S7. UV-visible absorption spectra obtained from the samples in Fig. S6 before (black curve) and after (red one) applying a GDR at a fixed solution concentration of 10^{-4} M for 30 min. The inset is the magnified view around the characteristic Au peak.

In general, the LSPR band of noble metal nanostructures shows red shift behavior upon increasing the dielectric constant. Here, this effect is marginally observed because the thickness of the polymer shell around the metal NP is too thin (compare the Figure 2(b) and Fig. S7 for your information) .
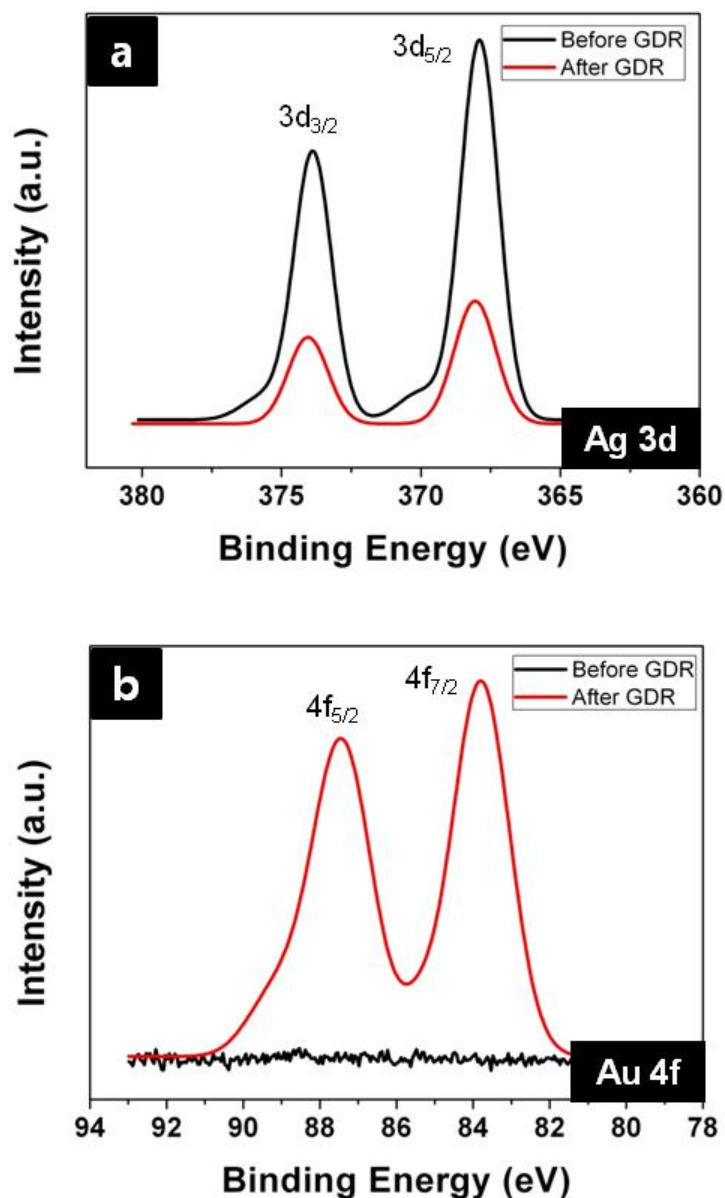
Figure S8. High resolution XPS spectra of (a) Ag$_{3d}$ and (b) Au$_{4f}$ obtained from the resultant NP arrays after GDRs embedded in the polymer shell in Fig. S6(c).

The XPS results show that the characteristic peak of Ag is still seen after GDRs, indicating that the reaction does not proceed as fast as the situation without polymer shell presumably due to retarded diffusion rate of the precursors.
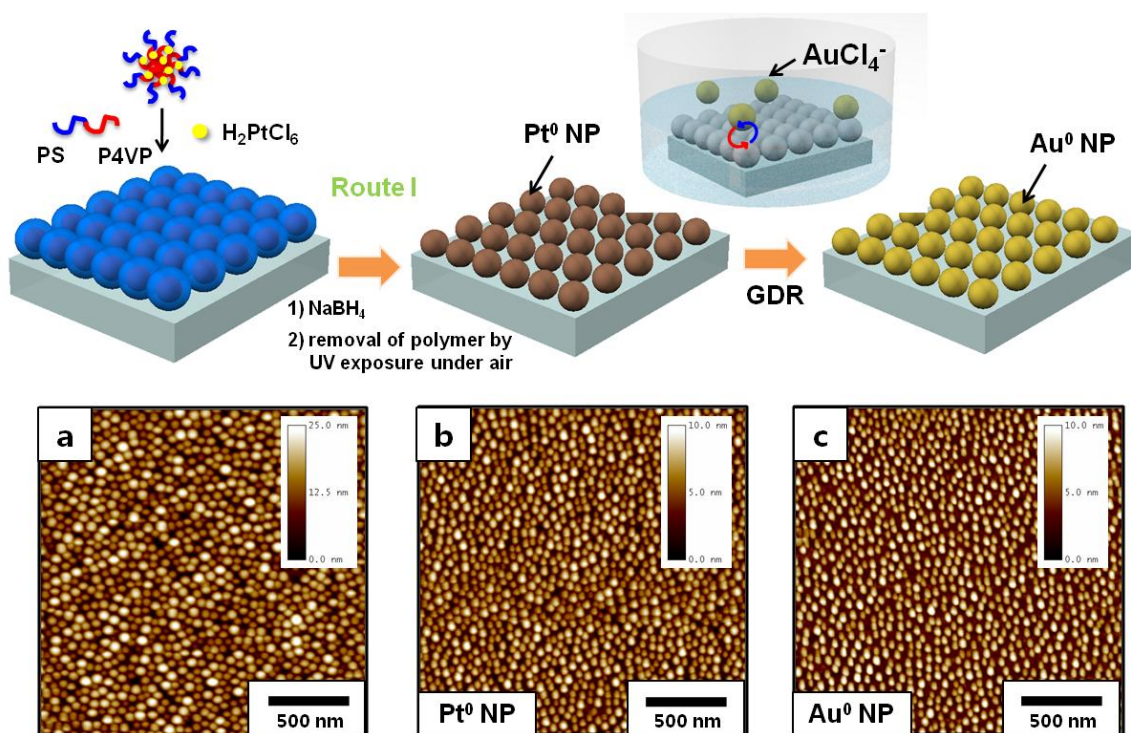
Figure S9. (upper panel) Schematic representation of the process to generate Au NP arrays by converting neat Pt NPs to Au NPs by applying GDRs. (bottom panel) (a) Height contrast AFM images of a PS-*b*-P4VP inverse micelle monolayer containing H_2PtCl_6 in the P4VP core; (b) Pt NP arrays obtained by exposing the identical film in Fig. S9(a) to UV light in air during which polymer matrix is eliminated; (c) Au NP arrays obtained by applying a GDR on the Pt NP arrays in Fig. S9(b).